

RESEARCH ARTICLE

Enrichment of progenitor cells by 2-acetylaminofluorene accelerates liver carcinogenesis induced by diethylnitrosamine in vivo

María Paulette Castro-Gil¹  | Ricardo Sánchez-Rodríguez^{2,3}  |
 Julia Esperanza Torres-Mena¹  | Carlos David López-Torres¹  |
 Valeria Quintanar-Jurado¹ | Nayeli Belem Gabiño-López¹  |
 Saúl Villa-Treviño⁴  | Luis del-Pozo-Jauner⁵  | Jaime Arellanes-Robledo^{1,6}  |
 Julio Isael Pérez-Carreón¹ 

¹Laboratory of Liver Diseases, National Institute of Genomic Medicine, Ciudad de México, Mexico

²Foundation Istituto di Ricerca Pediatrica-Città della Speranza, Padova, Italy

³Department of Biomedical Sciences, University of Padova, Padova, Italy

⁴Department of Cell Biology, Center for Research and Advanced Studies of the National Polytechnic Institute, Ciudad de México, Mexico

⁵Department of Pathology, University of South Alabama, Alabama, USA

⁶Directorate of Cátedras, National Council of Science and Technology, Ciudad de México, Mexico

Correspondence

Julio Isael Pérez-Carreón, Instituto Nacional de Medicina Genómica, Periférico Sur No. 4809, Col. Arenal Tepepan, Delegación Tlalpan, D.F.C.P., 14610 Ciudad de México, México.
 Email: jiperez@inmegen.gob.mx

Funding information

CONACYT-Mexico, Grant/Award Numbers: CB-182450, 85552; Instituto Nacional de Medicina Genómica, Grant/Award Number: #403

Abstract

The potential role of hepatocytes versus hepatic progenitor cells (HPC) on the onset and pathogenesis of hepatocellular carcinoma (HCC) has not been fully clarified. Because the administration of 2-acetylaminofluorene (2AAF) followed by a partial hepatectomy, selectively induces the HPC proliferation, we investigated the effects of chronic 2AAF administration on the HCC development caused by the chronic administration of the carcinogen diethylnitrosamine (DEN) for 16 weeks in the rat. DEN + 2AAF protocol impeded weight gain of animals but promoted prominent hepatomegaly and exacerbated liver alterations compared to DEN protocol alone. The tumor areas detected by γ -glutamyl transferase, prostaglandin reductase-1, and glutathione S-transferase *Pi*-1 liver cancer markers increased up to 80% as early as 12 weeks of treatment, meaning 6 weeks earlier than DEN alone. This protocol also increased the number of Ki67-positive cells and those of CD90 and CK19, two well-known progenitor cell markers. Interestingly, microarray analysis revealed that DEN + 2AAF protocol differentially modified the global gene expression signature and induced the differential expression of 30 genes identified as HPC markers as early as 6 weeks of treatment. In conclusion, 2AAF induces the early appearance of HPC markers and as a result, accelerates the hepatocarcinogenesis induced by DEN in the rat. Thus, since 2AAF simultaneously administrated with DEN enriches HPC during hepatocarcinogenesis, we propose that DEN + 2AAF protocol might be a useful tool to investigate the cellular origin of HCC with progenitor features.

KEYWORDS

cancer biomarkers, cellular origin of liver cancer, cirrhosis, hepatocellular carcinoma, liver progenitor cells, oval cells

María Paulette Castro-Gil, Ricardo Sánchez-Rodríguez, Julia Esperanza Torres-Mena, and Carlos David Lopez-Torres contributed equally to this work.

This is an open access article under the terms of the Creative Commons Attribution-NonCommercial-NoDerivs License, which permits use and distribution in any medium, provided the original work is properly cited, the use is non-commercial and no modifications or adaptations are made.

© 2021 The Authors. *Molecular Carcinogenesis* published by Wiley Periodicals LLC.

1 | INTRODUCTION

Hepatocellular carcinoma (HCC) is frequently associated with cirrhosis and is one of the five most lethal neoplasms worldwide.¹ Animal models have played a key role in identifying both the molecular and cellular alterations throughout hepatocarcinogenesis progression.^{2,3} Following chronic liver injuries, hepatocyte and hepatic progenitor cells (HPC) give rise to HCC *in vivo*.⁴⁻⁶ Two possibilities have been proposed to explain the progenitor features of HCC, either the hepatocyte dedifferentiation or transformation into neoplastic cells and the cancer-initiation by HPC. In normal liver, HPC are originated from canals of Hering in the periportal region and might be identified by progenitor markers, such as CD90, CK19, and OV-6.⁷

The Solt and Farber HCC model, also referred as the “resistant hepatocyte model,” induces the HCC along with the expression of progenitor cell markers in 9 months after a single intraperitoneal (i.p.) injection of the carcinogen diethylnitrosamine (DEN), 2-acetylaminofluorene (2AAF) in the diet and finally, a partial hepatectomy (PH) as the proliferative stimulus for liver regeneration.⁸ In this protocol, the combination of 2AAF with PH is the key intervention for the HPC activation during liver regeneration in the rat.⁹ For this ending, the hepatocytes DNA is preferentially cross-linked by 2AAF to prevent their proliferation, and as a result, HPC niches are expanded by the hepatic regeneration stimulus. The molecular mechanism that places 2AAF as a hepatocytes-specific anti-mitotic agent is the cytochrome p450 (CYP)-dependent metabolic activation of 2AAF that forms N-hydroxy-2AAF.^{10,11}

DEN is a liver carcinogen that induces a high incidence of HCC in rodents.¹² The Schiffer hepatocarcinogenesis model consists of the weekly i.p. injection of DEN that induces cirrhosis and multifocal HCC in only 18 weeks.¹³ It has been shown that DEN can also cause HCC bearing positive HPC markers, including OV-6 and CD133, which are mediated by transforming growth factor β (TGF- β) participation.¹⁴ Thus, by considering first that DEN induces HCC but at the same time activates progenitor cell markers and second, that 2AAF selectively promotes the HPC proliferation, we hypothesized that the chronic administration of DEN plus 2AAF accelerates the HCC progression by inducing the preferential activation of the HPC proliferation without the PH intervention in the rat. By measuring histopathological alterations, HCC and HPC markers, cell proliferation, and global gene expression changes, we provide evidence that the chronic administration of 2AAF and DEN enriches the hepatocarcinogenesis process with HPC resulting in liver tumors bearing progenitor cell features.

2 | MATERIALS AND METHODS

2.1 | Experimental procedures

Animals were obtained from the Production Unit of Experimental Laboratory Animals at UPEAL-CINVESTAV. Forty male Fisher 344

rats weighing 180–200 g (6–8 weeks old) were randomly divided into two groups for the DEN-induced HCC with or without the administration of 2AAF. For DEN and DEN + 2AAF protocols, DEN was weekly i.p. injected at 50 mg/kg,¹³ but for DEN + 2AAF protocol, animals were additionally subjected to the oral administration of 2AAF at 25 mg/kg three days after each DEN injection (Figure 1A). All experiments were performed according to the committee guidelines and the institutional-approved protocols for animal care under the number 0001-02. Additionally, eight animals were administered with saline solution and 15 animals were weekly administered with 2AAF, as the normal liver group (NL) and as the 2AAF control (2AAF group), respectively. For oval cell induction, five animals received 2AAF for 3 days before the intervention of 70% partial hepatectomy (2AAF + PH group), and then livers were resected 2 weeks later. For euthanasia, animals were exsanguinated from inferior vena cava under ether anesthesia. Livers were excised, washed in saline solution, frozen in 2-methyl butane with liquid nitrogen, and stored at -70°C for further analyses.

2.2 | Histological examination

Sections of liver tissues were fixed in 4% formaldehyde, dehydrated, and embedded in paraffin. Five-micron-thick sections were cut and stained with Hematoxylin & Eosin or Masson's trichrome according to conventional protocols for detecting histopathological alterations. Description of histopathological scoring (Table 1 and Table S1) was performed in a blinded manner by a pathologist.

2.3 | Detection of tumor and proliferation markers by histochemistry and immunohistochemistry analyses

The histochemistry analysis was used for detecting the tumor marker γ -glutamyl transferase (GGT), while immunohistochemistry analysis was used for detecting the tumor markers prostaglandin reductase-1 (PTGR1) and glutathione S-transferase *Pi*-1 (GSTP1), as well as, active Caspase-3, as previously described,¹⁵ by using commercial antibodies against PTGR1 (NovusBio), GSTP1 (Sigma-Aldrich), and cleaved Caspase-3 (Abcam). Images were captured with a microscope AXIO scope (Carl Zeiss). ImageJ plugins¹⁶ were used to quantitatively analyze the positive label in five images per animal and at least three animals per group.

2.4 | Immunofluorescence analysis

Liver sections were cut at 5-micron-thick from frozen tissue, fixed with acetone for 5 min at -20°C , blocked with 10% bovine serum albumin for 1 h, and then incubated overnight with anti-Laminin or anti-Ki67 (both at 1:100; Cell Marque). For double-detection of markers, anti-CD90 (1:50; NovusBio) was incubated

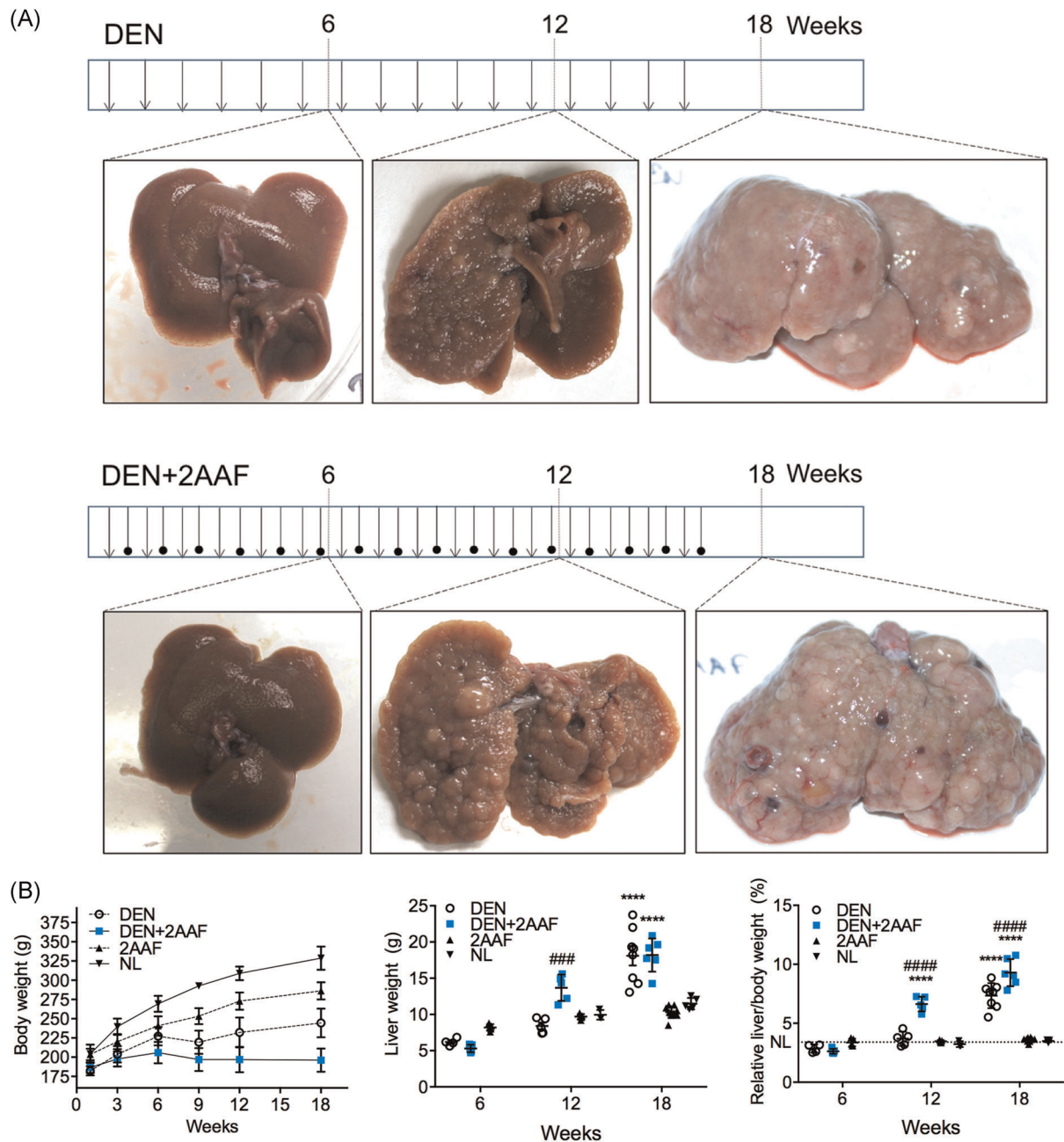


FIGURE 1 Comparison of hepatocarcinogenesis protocols in the rat. (A) Administration schemes of DEN and DEN + 2AAF protocols, including representative liver pictures at 6, 12, and 18 weeks. DEN protocol, arrows indicate the administration of DEN at 50 mg/Kg weekly. DEN + 2AAF protocol, similar to DEN protocol plus 2AAF at 25 mg/Kg, was orally administered three days after DEN (lines with a black dot). (B) Body weight of experimental groups. Non-cancer groups were both the 2AAF and normal liver (NL) groups. Liver weight and relative liver/body weight at 6, 12, and 18 weeks. Data mean \pm SD with **** p < .0001 compared to NL group. ### p < .001 and #### p < .0001 compared to DEN protocol at the respective week. 2AAF, 2-acetylaminofluorene; DEN, diethylnitrosamine [Color figure can be viewed at wileyonlinelibrary.com]

overnight, and anti-CK19 (1:100; Bio SB) was only incubated for 1 h in the same tissue section after removing and washing the first antibody. Primary antibodies were detected using either anti-mouse (Alexa 488) or antirabbit (Alexa 594), respectively (both at 1:300; Jackson) for 1 h. As an experimental control, the

substitution of the primary antibody with either mouse or rabbit isotype control was also included. Images were captured with a microscope AXIO scope (Carl Zeiss). ImageJ plugins¹⁶ were used to quantitatively analyze the positive label in five images per animal and at least three animals per group.

TABLE 1 Histologic alterations induced by DEN and DEN + 2AAF protocols

Histological parameter	DEN (weeks)			DEN + 2AAF (weeks)		
	6	12	18	6	12	18
Hyperplasia	-	+	+	+		+
Dysplasia	-	+	+	+	+	+
Cancer cell	-	-	+	-	+	+
			(W-D/MD)		(W-D/MD)	(W-D/MD)
Cellular infiltration	1	1	1	1	1	1
Fibrosis	1	2	2/3	1	2	2/3
Oval cells	0	1	1	0	1	1
Ballooning degeneration	1	1	1	1/2	1	1
Steatosis	0	0	0	0	0	1
Cholestasis	0	1	1	1	1	0
Mallory bodies	0	0	0	0	0	0/1
Lobular inflammation	0	0	0	0	0	0
Periportal bile ducts proliferation	0	1	1/2	0/1	1	1/2

Note: Pathologic score was assigned: 0 = none, 1 = mild, 2 = moderate, 3 = large, + = present, and - = absent.

Abbreviations: 2AAF, 2-acetylaminofluorene; DEN, diethylnitrosamine; HCC, hepatocellular carcinoma; MD, moderate-differentiated HCC; WD, well-differentiated HCC.

2.5 | Western blot analysis

Total protein extracts were obtained with radio-immunoprecipitation assay buffer. Thirty milligrams of proteins were analyzed through sodium dodecyl sulfate polyacrylamide gel electrophoresis and transferred to polyvinylidene difluoride membranes (Millipore) by electroblotting. Membranes were blocked in 10% albumin and then incubated overnight at 4°C with either anti-GSTP1 (Sigma-Aldrich), anti-Actin (Abcam), or anti-PTGR1 (NovusBio) primary antibodies, at 1:1000 dilution. After washing, membranes were incubated with an anti-rabbit peroxidase-conjugated secondary antibody (Jackson). Protein complexes were detected with chemiluminescence using the Immobilon Western Chemiluminescent HRP Substrate (Millipore). Images were obtained with a chemiluminescence imaging system (Uvitec).

2.6 | Quantitative reverse transcription polymerase chain reaction analysis

Total RNA was obtained from 30 mg of frozen tissue by using RNeasy miniKit (Qiagen). Complementary DNA (cDNA) reactions were performed from 750 ng of total RNA using High-Capacity

cDNA Reverse Transcription Kit (Thermo Fisher Scientific Inc.). Polymerase chain reaction (PCR) reactions were carried out using TaqMan gene expression assays using the ViiA7 Real-Time PCR System. FAM dye-labeled probes for rat *Gstp1* (Rn00561378 gH), *Ptgr1* (Rn00593950 m1), *Col1a1* (Rn01463848_m1), *Tgfb* (Rn01475963_m1), and *18S rRNA* (Rn03928990) were acquired from Applied Biosystems. Data were normalized with *18S rRNA* gene expression using the comparative $\Delta\Delta C_t$ method.¹⁷

2.7 | Microarray analysis

Rat Gene 1.0 ST Affymetrix arrays were used for evaluating the whole-transcript expression profiling. Microarray analysis was performed at the INMEGEN microarrays core facility and all procedures were according to Affymetrix's protocol. Briefly, double-strand cDNA was obtained from total RNA using Superscript II reverse transcriptase with poly(T) oligomer. Then, cDNA served as a template for generating biotin-labeled cRNA. The GeneChip hybridization Oven 645 (Affymetrix) provided controlled temperature and rotation for hybridization for 17 h at 45°C. After hybridization, arrays were washed and stained by using streptavidin-phycoerythrin in an Affymetrix Fluidics Station 450 (Affymetrix). Then, microarrays were scanned by GeneChip Scanner 3000 7G (Affymetrix). Data normalization was performed by using the transcriptome analysis Console 4.0 software (Robust Microarray Average algorithm; Thermo Fisher Scientific Inc.) and differential gene expression analysis (fold change cut-off ± 2 , analysis of variance [ANOVA], $p \leq .05$). The R ggplot2 library was used to generate plots of principal component analysis (PCA). Intergroup hierarchical clustering was performed by using IBM SPSS Statistics (IBM) using total normalized microarray expression. ClustVis software was used to construct the heat map graphic of differentially expressed genes.

2.8 | Statistical analysis

Results were expressed as mean \pm SD. Significance was determined by one-way ANOVA and Sidak's multiple comparisons test. Statistical significances were obtained by comparing DEN + 2AAF protocol with the same time-matched of DEN protocol; as well as, these protocols to NL control. Statistical significance was defined as a $p < .05$.

3 | RESULTS

3.1 | The addition of 2AAF to DEN-induced HCC protocol exacerbates hepatomegaly and nodular appearance

It is well established that chronic administration of DEN alone induces progressive carcinogenesis in the liver. Here, we show that livers exposed to DEN showed a slightly rough surface at 6 weeks, a cirrhotic

appearance at 12 weeks, and several HCC nodules were evident at 18 weeks (Figure 1A). Both the number and size of nodules were more remarkable by DEN + 2AAF protocol than those induced by DEN alone on the liver surface at 12 and 18 weeks. Livers also showed necrotic areas and multiple tumors at 18 weeks. Animals subjected only to 2AAF did not develop neoplastic nodules (Figure S1 and Table S1). Animal body weights were increasingly affected by the different protocols as follows 2AAF, DEN, and the combination DEN + 2AAF (Figure 1B). Moreover, animals subjected to DEN + 2AAF protocol exhibited an exacerbated hepatomegaly after 12 weeks of treatment; this phenomenon was evidenced by 7% ($p < .0001$) increment in the relative liver/body weight ratio, whereas animals subjected to DEN protocol showed only 4% increment. DEN and DEN + 2AAF protocols produced hepatomegaly at 18 weeks, and the relative liver/body weight reached 9% in those animals subjected to DEN + 2AAF protocol and 7.2% in those subjected to DEN alone. Thus, the incorporation of 2AAF in a well-known DEN-induced HCC protocol produces hepatomegaly and HCC nodules from 12 weeks of administration.

3.2 | DEN + 2AAF protocol induces earlier HCC-associated alterations than DEN alone

Histopathological alterations detected by hematoxylin and eosin staining (Table 1 and Figure S2) showed that DEN protocol induced hyperplasia and dysplasia at 12 and 18 weeks, as well as, well- and moderately-differentiated HCC at 18 weeks. While DEN + 2AAF protocol induced early hyperplasia from 6 to 18 weeks and well- and moderately-differentiated HCC from 12 to 18 weeks; that is, 6 weeks before than DEN protocol. During the time-course experiment, both protocols induced a mild chronic type of cellular infiltration. Livers showed cholestasis, mild ballooning degeneration, and oval cells induced by both protocols from 12 to 18 weeks. The only alteration induced by 2AAF alone was a slight ballooning degeneration (Table S1). DEN + 2AAF protocol induced microvesicular steatosis and Mallory bodies at 18 weeks. Finally, the proliferation of periportal bile duct cells was induced by both protocols, but DEN + 2AAF protocol induced it as early as 6 weeks after the initial administration.

3.3 | DEN + 2AAF protocol promotes fibrogenesis at similar levels than DEN protocol and induces early expression of *Tgfb1* gene

Both HCC protocols promoted fibrogenesis as measured by two fibrosis biomarkers; collagen and laminin.¹⁸ Masson's trichrome staining (Figure 2A) and immunohistochemistry analysis (Figure 2B) showed that these protocols similarly increased both the collagen and laminin liver contents, respectively, as compared to NL group. To determine further alterations induced by these protocols, we measured the expression of two key genes involved in liver fibrogenesis, namely *Col1a1*, which encodes collagen type 1, and *Tgfb1*, its main regulator.¹⁹ The last gene

encodes for TGF- β , a central activator of hepatic stellate cells and HPCs in DEN-induced rat hepatocarcinogenesis.¹⁴ *Col1a1* messenger RNA (mRNA) expression was increased more than 110 fold change (FC) from 12 to 18 weeks ($p < .01$ and $p < .05$, respectively) by DEN + 2AAF protocol; in contrast, DEN protocol did not induce statistically significant *Col1a1* mRNA expression (Figure 2C). *Tgfb1* mRNA expression was significantly increased (>9 FC, $p < .05$) at 18 weeks by DEN protocol, while DEN + 2AAF protocol induced the highest *Tgfb1* mRNA expression (>12 FC, $p < .01$) as early as 6 weeks, and its expression remained at that level until 18 weeks ($p < .01$). Although both protocols similarly promoted the fibrogenesis as observed histologically, the DEN + 2AAF protocol induced higher *Col1a1* mRNA levels at 12 and 18 weeks ($p < .05$) and higher *Tgfb1* mRNA levels at 6 and 12 weeks ($p < .01$) than DEN protocol.

3.4 | DEN + 2AAF protocol accelerates HCC development

To follow the hepatocarcinogenesis progression, we determined the expression of GGT, PTGR1, and GSTP1, three well-known HCC biomarkers (Figure 3).^{15,20} The levels of all three markers were clearly different after 6 weeks of treatments in both protocols. DEN + 2AAF protocol induced altered hepatocyte foci (AHF), reaching up to 0.43 mm diameter. The AHF size reached a maximum diameter of 0.16 mm by DEN protocol (Figure 3A). The percentage of GGT-positive tissue was induced 19% higher ($p < .001$) by DEN + 2AAF protocol than DEN alone at 6 weeks, 40% ($p < .001$) at 12 weeks, and 12% ($p < .01$) higher at 18 weeks of treatment

(Figure 3B). We have previously described that PTGR1 is a useful rat hepatocarcinogenesis marker.¹⁵ Figure 3C shows that DEN + 2AAF protocol induced bigger PTGR1-positive nodules at 6 and 12 weeks than DEN protocol. *Ptgr1* mRNA level showed a gradual increment at 12 and 18 weeks (16 and 18 FC respectively, $p < .01$) by DEN protocol; however, this expression reached its highest level at 12 weeks (28 FC, $p < .001$) and slightly decreased at 18 weeks (18 FC, $p < .01$) (Figure 3D) by DEN + 2AAF protocol. Protein and mRNA levels of PTGR1 were similarly induced by both protocols (Figure 3G). One of the most sensitive markers used in the rat hepatocarcinogenesis models is GSTP1.²¹ DEN + 2AAF protocol induced more GSTP1-positive nodules at 6 and 12 weeks than DEN protocol (Figure 3E). Although *Gstp1* mRNA expression levels were not statistically different between both HCC protocols, DEN + 2AAF protocol induced its highest level at 12 weeks (430 FC compared to NL $p < .01$) (Figure 3F). Western blot analyses revealed that GSTP1 protein level was induced from 6 weeks by DEN + 2AAF but not by DEN protocol (Figure 3G). Together, these results confirm that DEN + 2AAF protocol accelerates the hepatocarcinogenesis progression.

3.5 | DEN + 2AAF and DEN protocols increase proliferation and cell death ratios

To investigate whether proliferation and cell death were critical players in the accelerated HCC progression, we measured these processes by

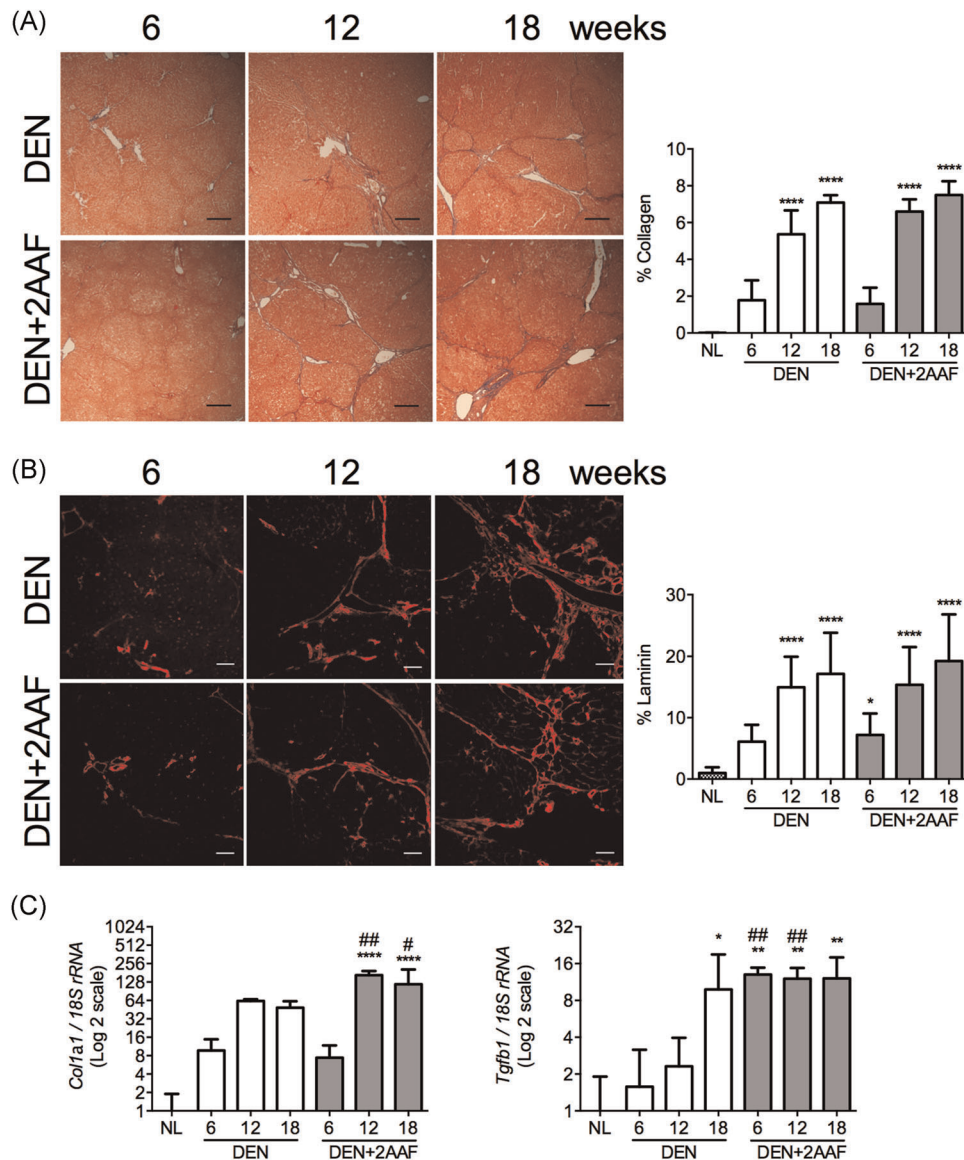


FIGURE 2 DEN and DEN + 2AAF protocols induce similar fibrogenesis. (A) Representative images of Masson's trichrome staining, Magnification $\times 50$. Fibers quantification (blue) reveals increased collagen by the HCC protocols at 6, 12, and 18 weeks. (B) Representative IF images for Laminin (Red) and quantification of the laminin-positive tissue. Magnification $\times 100$. (C) Relative gene expression of *Col1a1* and *Tgfb1* mRNA normalized to 18S rRNA. Data corresponded to mean \pm SD. * $p < .05$, ** $p < .01$, **** $p < .0001$ compared to NL. # $p < .05$ and ## $p < .01$ compared to DEN protocol at the respective week. 2AAF, 2-acetylaminofluorene; DEN, diethylnitrosamine; IF, immunohistochemistry; rRNA, ribosomal RNA; NL, normal liver [Color figure can be viewed at wileyonlinelibrary.com]

determining the number of Ki67- and Caspase-3-positive cells (Figure 4). Both DEN and DEN + 2AAF protocols gradually increased the number of Ki67-positive cells from 6 to 18 weeks ($p < .05$ to $p < .0001$, respectively). Remarkably, DEN + 2AAF protocol induced a maximum peak of Ki67-positive cells at 12 weeks (Figure 4A,B) by increasing 14% ($p < .05$) the label of Ki67-positive cells than DEN protocol. Immunolabeling of Caspase-3 revealed that both protocols gradually increased the cell death ratio, but no one showed statistical differences between each other (Figure 4C,D). Our result indicates that both cell proliferation and apoptosis increased ratios denote a relevant cell turnover through the HCC progression.

3.6 | DEN + 2AAF protocol promotes the early increase of HPC

Then, we investigated whether the appearance of HPC is associated with the accelerated progression of HCC; for this end, we detected the HPC markers CD90 and CK19 in the liver tissue. First, we induced HPC proliferation in the rat liver by using the 2AAF + PH protocol as a positive control.¹⁵ Animals subjected to this procedure showed copious clusters of CD90- and CK19-positive cells in the whole liver; in contrast, the HPC markers were only detected surrounding bile ducts in portal tracts in the

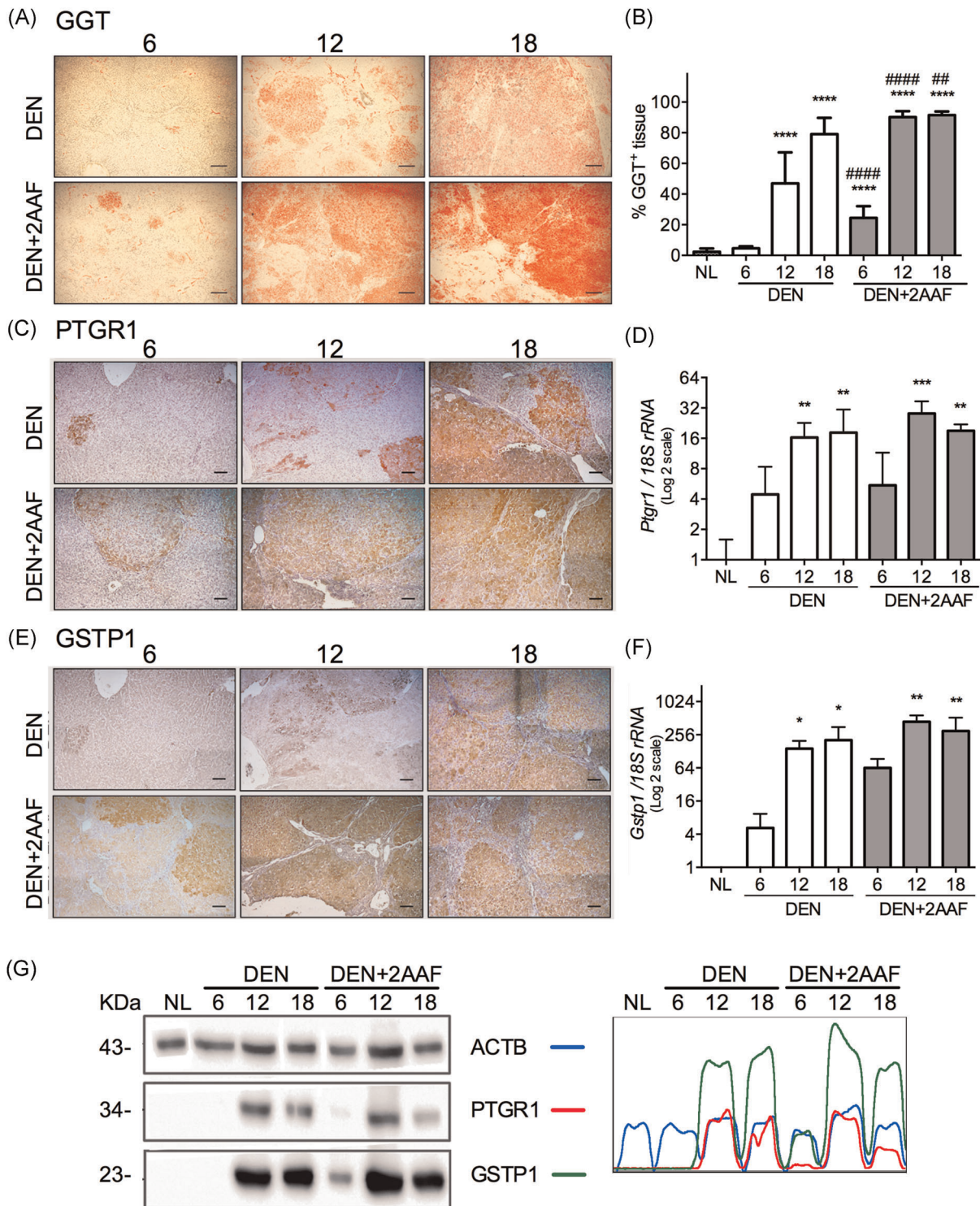


FIGURE 3 DEN + 2AAF protocol accelerates liver carcinogenesis. (A) Representative images showing GGT detection in liver tissues from DEN and DEN + 2AAF protocols at 6, 12, and 18 weeks. Magnification $\times 50$. (B) Percentage of GGT-positive tissue. (C) Representative IHC images for PTGR1. Magnification $\times 100$. (D) Expression of *Ptgr1* mRNA normalized to *18S rRNA* determined by reverse transcription polymerase chain reaction (RT-PCR). (E) Representative IHC images for GSTP1. Magnification $\times 100$. (F) Expression of *Gstp1* mRNA normalized to *18S rRNA* determined by RT-PCR. (G) Representative western blot analysis for PTGR1 and GSTP1 (left) and densitometric analysis of blots (right). Data were presented as mean \pm SD. with $*p < .05$, $**p < .01$, $***p < .001$, $****p < .0001$ compared to NL group. $\#p < .01$ and $####p < .0001$ compared to DEN protocol at the respective week. 2AAF, 2-acetylaminofluorene; DEN, diethylnitrosamine; GGT, γ -glutamyl transferase; IHC, immunohistochemistry; mRNA, messenger RNA; rRNA, ribosomal RNA; NL, normal liver [Color figure can be viewed at wileyonlinelibrary.com]

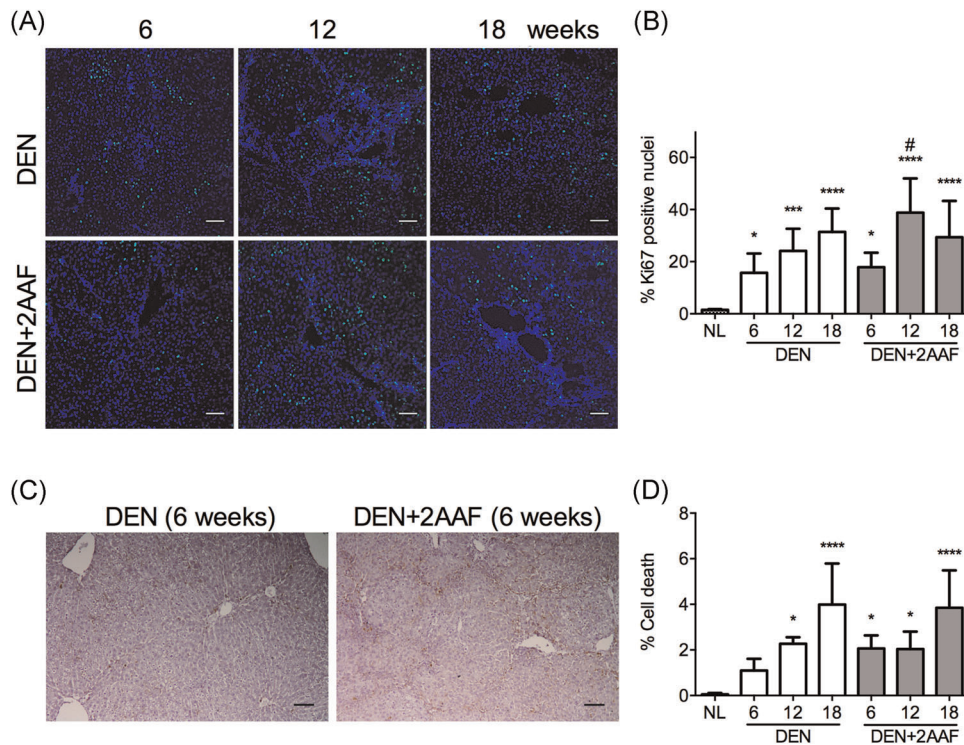


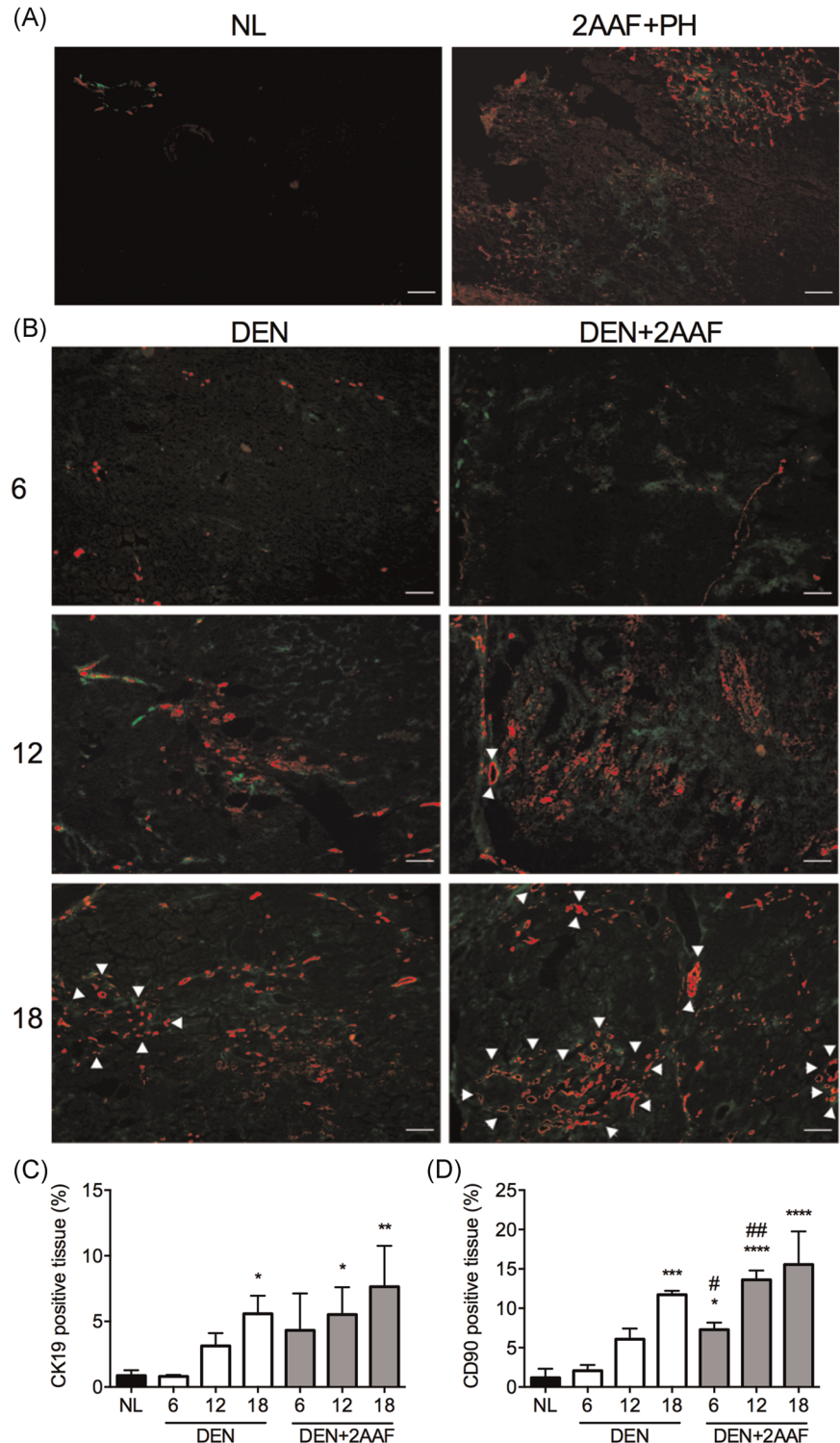
FIGURE 4 Proliferation and cell death induced by DEN and DEN + 2AAF protocols. (A) Representative IF images for Ki67 antigen (green). Nuclei were stained with DAPI (blue). Magnification $\times 100$. (B) Percentage of proliferative cells (Ki67-positive cells). (C) Representative IHC images for detecting active Caspase-3. (D) Percentage of cell death detected by active Caspase-3. Data were presented as mean \pm SD with * $p < .05$, ** $p < .001$, **** $p < .0001$ compared to NL group. # $p < .05$ compared to DEN group at the respective week. 2AAF, 2-acetylaminofluorene; DAPI, 4',6-diamidino-2-phenylindole; DEN, diethylnitrosamine; IF, immunohistochemistry; IHC, immunohistochemistry; NL, normal liver [Color figure can be viewed at wileyonlinelibrary.com]

liver of untreated animals (Figure 5A). The expression of CD90 and CK19 gradually increased from 6 to 18 weeks by both HCC protocols (Figure 5B). A critical HCC prognostic marker that involves HPC expansion is ductular reaction (DR) in the liver.²² The DR was noticeably observed along with the CK19 labeling, starting at 12 weeks and persisting until 18 weeks in animals subjected to DEN + 2AAF protocol (arrowheads, Figure 5B). DEN protocol induced DR only at 18 weeks but the levels of CK19 progressively augmented, reaching 5.57% ($p < .05$) at 18 weeks of treatment. However, the percentage of CK19-positive tissue was increased by 5.52% ($p < .05$) at 12 weeks and 7.64% ($p < .01$) at 18 weeks by DEN + 2AAF protocol (Figure 5C). Remarkably, DEN + 2AAF protocol induced the early emerging of CD90-positive cells that represented 7% and 13% ($p < .05$, $p < .01$ compared to NL and DEN group, respectively) at 6 and 12 weeks, respectively; but it reached its highest level at 18 weeks (15%, $p < .0001$ compared to NL group) (Figure 5D). Taken together, these results indicate that the increased induction of CD90- and CK19-positive cells by DEN + 2AAF protocol is associated with the accelerated HCC progression.

3.7 | DEN + 2AAF protocol induces an HPC-associated gene expression signature earlier than DEN protocol

We then performed a microarray analysis to identify a specific gene expression signature associated with a progenitor cell phenotype in both HCC protocols. PCA showed a clear separation among groups according to the experimental HCC progression (Figure 6A). Interestingly, animals from DEN + 2AAF protocol showed a different position than those in DEN protocol. As early as 6 weeks of DEN + 2AAF treatments, animals were clearly separated from DEN treatment. Of note, there was spatial overlap in DEN + 2AAF-treated animals at 12 and 18 weeks, but they were far from those treated for 6 weeks (Figure 6A). Coincidentally, the hierarchical clustering showed a differential gene expression profile between samples from DEN + 2AAF (cluster 2), while NL and DEN groups formed the cluster 1 (Figure 6B). Then, we selected those genes already reported as HPC markers (Table S2).²³ Gene expression analyses also provided evidence showing the early appearance of HPC markers by DEN + 2AAF protocol. Figure 6C illustrates that 30 genes

FIGURE 5 CD90 and CK19 progenitor cell markers are increased by DEN + 2AAF protocol. Representative IF image for CD90 (green) and CK19 (red) in (A) NL and 2AAF plus partial hepatectomy (PH) as a positive control for HPC markers. (B) DEN and DEN + 2AAF protocol at 6, 12, and 18 weeks. Magnification of $\times 100$. (C, D) Quantitative analysis of CK19- and CD90-positive tissue, respectively, in DEN and DEN + 2AAF protocols. Data were presented as mean \pm SD with $*p < .05$, $**p < .01$, $***p < .001$, $****p < .0001$ compared to NL group. $\#p < .05$, $##p < .01$ compared to DEN protocol at the respective week. 2AAF, 2-acetylaminofluorene; DEN, diethylnitrosamine; HPC, hepatic progenitor cell; IF, immunofluorescence; NL, normal liver [Color figure can be viewed at wileyonlinelibrary.com]



identified as HPC markers were differentially expressed from 6 weeks but their expression was exacerbated at 12 and 18 weeks by DEN + 2AAF protocol. Hierarchical clustering analysis formed two clusters. While cluster 1 grouped all samples from 6 to 18 weeks of DEN + 2AAF protocol, cluster 2 included samples of NL and DEN protocol. Figure S3A and Table S2 show the number of genes statistically different ($p < .05$) among the 30 HPC markers. DEN + 2AAF protocol induced a higher number of genes than DEN protocol, but

this difference was more remarkable at 6 weeks of treatment. Figure S3B,C show that *Krt19* (CK19) and *Thy1* (CD90) mRNA expression (obtained from microarrays data) was increased by DEN + 2AAF protocol at 6 weeks. These results confirm that the accelerated hepatocarcinogenesis induced by DEN + 2AAF protocol is associated with the appearance of an HPC-associated gene expression signature, which is detectable as early as 6 weeks of treatment. Figure 7 shows a comparison of the overrepresented

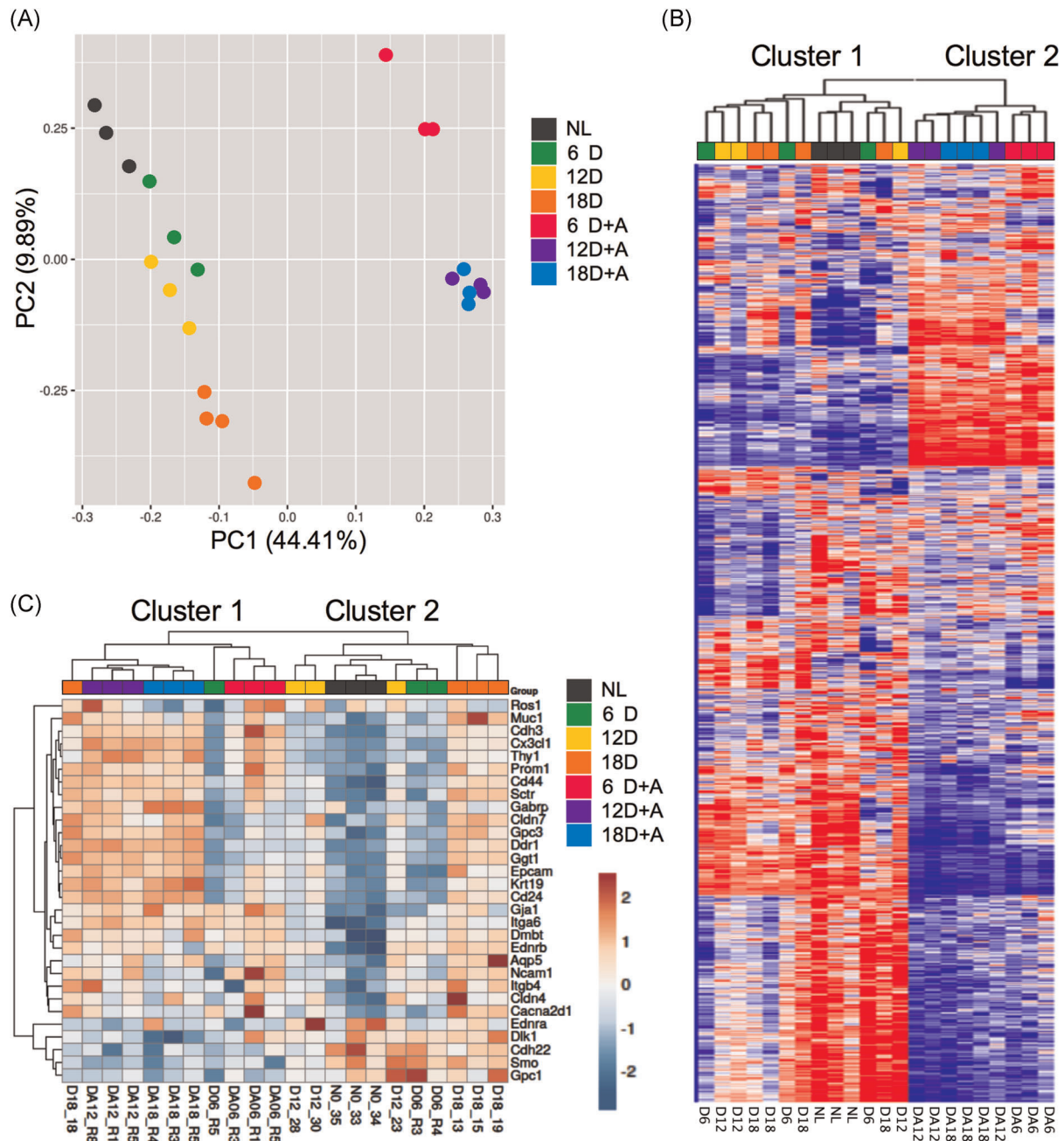


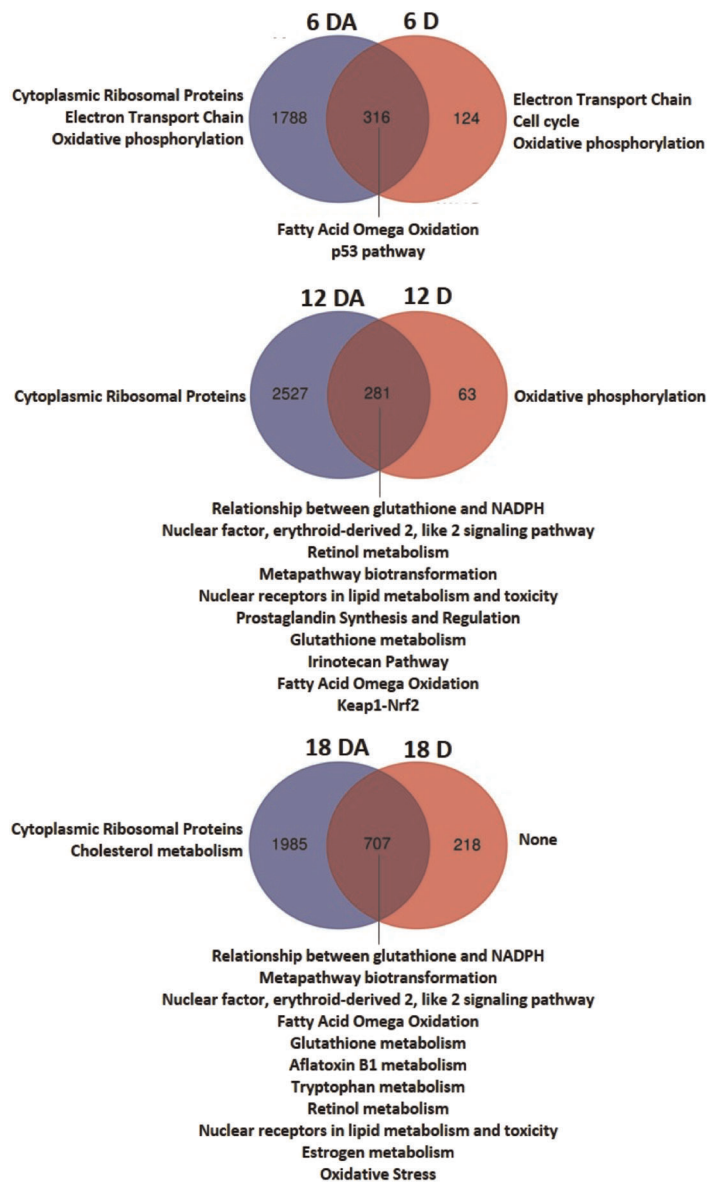
FIGURE 6 DEN + 2AAF protocol induces an HPC gene expression profile. (A) PCA of global gene expression profile after normalization. Each point represents a sample-specimen. NL, D (DEN protocol), D + A (DEN + 2AAF protocol) at 6, 12, or 18 weeks. (B) Heat map of differentially expressed genes. The dendrogram illustrates the hierarchical clustering of samples separated into two clusters. (C) Heat map showing transcript levels of selected genes identified as HPC markers. The dendrogram displays the hierarchical clustering of genes and samples split into two clusters. 2AAF, 2-acetylaminofluorene; DEN, diethylnitrosamine; HPC, hepatic progenitor cell; NL, normal liver; PCA, principal component analysis [Color figure can be viewed at wileyonlinelibrary.com]

pathways from the gene expression analysis of both HCC protocols. Both protocols provoked a time-associated increase of metabolic pathways, such as oxidative phosphorylation, electron transport chain, fatty acid, cholesterol, amino acid metabolism, and response to oxidative stress-mediated by the Keap1-NRF2 pathway. Remarkably, the cytoplasmic ribosomal proteins pathway was distinctive between DEN + 2AAF and DEN protocols from 6 to 18 weeks.

4 | DISCUSSION

Here, we have designed an alternative hepatocarcinogenesis model associated with cirrhosis that accelerates for up to 6 weeks earlier the HCC development, as compared to a DEN-induced HCC model, previously reported.¹³ In addition to DEN administration, this alternative model consisted of the administration of 2AAF, an inhibitor

FIGURE 7 Overrepresented pathways between DEN and DEN + 2AAF protocols. Venn diagrams show the number of differential genes and the main overrepresented pathways. D (DEN protocol), DA (DEN + 2AAF protocol) at 6, 12, or 18 weeks. 2AAF, 2-acetylaminofluorene; DEN, diethylnitrosamine; NADPH, nicotinamide adenine dinucleotide phosphate [Color figure can be viewed at wileyonlinelibrary.com]



of the hepatocyte proliferation that under a liver regeneration pressure, such as that produced by a PH, selectively induces the HPC proliferation.⁹ Both protocols induced similar fibrosis levels, as evaluated by the histological presence of collagen and laminin; however, the inclusion of 2AAF exacerbated the number of macroscopic HCC nodules, which were confirmed by the earlier appearance of the tumor markers GGT, PTGR1, and GSTP1. DEN + 2AAF protocol increased cell proliferation at 12 weeks and the percentage of CD90- and CK19-positive HPC within HCC nodules. Gene expression analysis confirmed the differences between HCC protocols, especially the early enrichment of HPC markers induced by DEN + 2AAF protocol. The differential expression of selected genes already reported as HPC markers²³ confirmed that accelerated HCC progression is associated with a progenitor cell phenotype induced by DEN + 2AAF protocol.

2AAF has shown a profound carcinogenic activity with a linear correlation at high cumulative doses, from 28.8 to 282 mg/kg,

and produces HCC at 200 mg/kg in the rat.²⁴ It is relevant to point out that 2AAF failed to induce a tumorigenic response by itself at 25 mg/kg. Thus, 2AAF induced minimal liver damage at this dose compared to DEN or DEN + 2AAF protocols (Figure S1). Evidently, the DEN + 2AAF protocol induced an elevated number of tumors and accelerated the appearance of GGT-positive nodules. It has been reported that 2AAF, combined with DEN, acts as a cancer promoter.²⁵⁻²⁷ The possible mechanism of action of 2AAF seems to depend on the CYP450 activity, which selectively suppresses the hepatocyte proliferation by modifying cell cycle-related genes, thereby leading to the HPC activation.^{11,28-30} Despite we have shown that DEN + 2AAF protocol increased 14% in cell proliferation at Week 12 compared to DEN group, a comparative measurement of cell proliferation and cell death between hepatocytes and HPC would better explain the accelerated HCC development promoted by DEN + 2AAF protocol. Thus, we believe that future measurement of cell proliferation

and apoptosis ratios at intermediate times, that is, at 6 and 12 weeks by using specific markers, may provide more accurate evidence of which of these cellular processes contribute to accelerating the tumor development.

HCC commonly emerges from pre-neoplastic cells in patients bearing cirrhosis for many years.³¹ Although there are many rodent models to recapitulate HCC, few reproduce the gradual appearance of both cirrhosis and HCC.³² Here, we showed that DEN + 2AAF protocol induces multinodular HCC associated with cirrhosis within 12 weeks, that is, 6 weeks earlier than the HCC model proposed by Schiffer (DEN protocol).¹³ DEN + 2AAF protocol induced bigger GGT-, PTGR1-, and GSTP1-positive HCC nodules 6 weeks earlier than DEN protocol. Interestingly, these tumor-markers are also expressed by progenitor cells; for example, the HPC and cholangiocytes express GGT in normal livers.³³ Moreover, PTGR1 has been found over-expressed in both CD90-positive HCC³⁴ and CK19-positive pre-neoplastic lesions in the rat.^{35,36}

Additionally, a simultaneous increment of HPC and TGF- β in DEN-induced hepatocarcinogenesis has been also described,¹⁴ a phenomenon that we observed at gene expression level at 18 weeks induced by DEN protocol (Figures 2D and 5C,D). DEN + 2AAF protocol induced *Tgfb1* mRNA expression from 6 to 18 weeks; accordingly, the HPC markers CD90 and CK19 showed a similar expression pattern that was higher than DEN protocol (Figures 2D and 5C,D, and Figure S3). The liver periportal region, where DR occurs, has been suggested as the HPC niche,²² and HPC proliferation has been correlated with the liver disease severity.³⁷ While DEN protocol induced DR only at 18 weeks, DEN + 2AAF protocol induced it from 12 weeks and exacerbated it at 18 weeks of treatment (Figure 5B). The simultaneous appearance of both phenomena named *Tgfb1* mRNA expression and DR, suggests that DEN + 2AAF protocol prompts the HCC development bearing progenitor cell features. Future research on the DEN + 2AAF protocol could clarify the molecular mechanism that involves the participation of TGF- β in the early induction of HPC, the relationship with the fibrogenic process, and tumor development.

The differential expression of 30 genes identified as HPC markers, the enrichment of CD90- and CK19-positive cells from 6 weeks, and the induction of tumors from 12 weeks by DEN + 2AAF protocol highlight the role of HPC as a source for neoplastic transformation. However, the capability of mature hepatocytes to undergo a dedifferentiation process,⁶ may also explain the remarkable intra-tumoral heterogeneity observed in DEN-induced hepatocarcinogenesis.³⁸ Based on our findings, we think that the hypotheses about the origin of HCC, that is, the hepatocyte dedifferentiation and the cancer-initiating role of HPC, are not mutually exclusive. Given the cellular complexity of tumor development in the liver, the tumors occurrence might result from the dedifferentiation process accompanied by HPC proliferation, occurring both in parallel and exacerbating the HCC progression.³⁹

Global gene expression data also provided clues on the metabolic pathways involved in liver carcinogenesis, such as oxidative phosphorylation, electron transport chain, fatty acid, cholesterol metabolism,

amino acid metabolism, and the Keap1-NRF2 pathway involved in oxidative stress-mediated response (Figure 7). These data could suggest the metabolic reprogramming in the tumoral cells, such as the Warburg effect and the reverse Warburg effect in the tumoral microenvironment.^{40,41} Also, lipid reprogramming could efficiently sustain the liver cancer stem cells.⁴² Remarkably, DEN + 2AAF protocol exclusively showed the cytoplasmic ribosomal proteins (RP) pathway over-represented (Figure 7). Dysregulation of RP expression has been associated with cell survival in cancers,⁴³ and the gene expression changes of RP have been identified in HPC during fetal development.⁴⁴ Thus, RP profile changes might represent and confirm a molecular signature for HCC that bears progenitor cell features. The gene expression data that we obtained in this investigation could be a starting point for developing new research lines that clarify the HPC participation in the HCC development.

5 | CONCLUSION

The simultaneous administration of 2AAF and DEN induces fibrosis and accelerates liver carcinogenesis accompanied by the enrichment of HPC markers. Thus, the DEN + 2AAF protocol represents a new tool for the study of multinodular HCC with progenitor cell features.

ACKNOWLEDGMENTS

María Paulette Castro Gil is a doctoral student from the Programa de Doctorado en Ciencias Biomédicas, Universidad Nacional Autónoma de México (UNAM) and has received CONACyT fellowship 741709. Authors thanks to Armando Cruz-Rangel, Raul Mojica Espinosa, José Luis Cruz-Colín, Ema Herrera-Lopez and Arely López-Hernández for the technical assistance at INMEGEN, and to Sergio Hernández-García for his technical assistance at CINVESTAV-IPN. This project was supported by INMEGEN (Grant number: 403) and CONACYT-Mexico (Grant number: CB-182450 and 85552).

CONFLICT OF INTERESTS

The authors declare that there are no conflict of interests.

ORCID

María Paulette Castro-Gil  <https://orcid.org/0000-0001-8670-1219>

Ricardo Sánchez-Rodríguez  <https://orcid.org/0000-0002-9111-2176>

Julia Esperanza Torres-Mena  <https://orcid.org/0000-0003-0514-5244>

Carlos David López-Torres  <https://orcid.org/0000-0002-8426-6193>

Nayeli Belem Gabiño-López  <https://orcid.org/0000-0002-3654-4961>

Saúl Villa-Treviño  <https://orcid.org/0000-0002-8292-8157>

Luis del-Pozo-Jauner  <https://orcid.org/0000-0002-2551-0301>

Jaime Arellanes-Robledo  <https://orcid.org/0000-0001-7363-4870>

Julio Isael Pérez-Carreón  <http://orcid.org/0000-0001-9284-7775>

REFERENCES

- Goutté N, Sogni P, Bendersky N, Barbare JC, Falissard B, Farges O. Geographical variations in incidence, management and survival of hepatocellular carcinoma in a Western country. *J Hepatol*. 2017;66(3):537-544.
- Li Y, Tang ZY, Hou JX. Hepatocellular carcinoma: insight from animal models. *Nat Rev Gastroenterol Hepatol*. 2011;9(1):32-43.
- De Minicis S, Kisseleva, Francis H, et al. Liver carcinogenesis: rodent models of hepatocarcinoma and cholangiocarcinoma. *Dig Liver Dis*. 2013;45(6):450-459.
- Alison MR, Islam S, NA. Wright, stem cells in cancer: instigators and propagators? *J Cell Sci*. 2010;123(Pt 14):2357-2368.
- Li J, Xin J, Zhang L, et al. Human hepatic progenitor cells express hematopoietic cell markers CD45 and CD109. *Int J Med Sci*. 2014;11(1):65-79.
- Kowalik MA, Sulas P, Ledda-Columbano GM, Giordano S, Columbano A, Perra A. Cytokeratin-19 positivity is acquired along cancer progression and does not predict cell origin in rat hepatocarcinogenesis. *Oncotarget*. 2015;6(36):38749-38763.
- Weiss TS, Dayoub R. Thy-1 (CD90)-positive hepatic progenitor cells, hepatocytes, and non-parenchymal liver cells isolated from human livers. *Methods Mol Biol*. 2017;1506:75-89.
- Michael AOA, Ahsan N, Zabala V, et al. Proteomic analysis of laser capture microdissected focal lesions in a rat model of progenitor marker-positive hepatocellular carcinoma. *Oncotarget*. 2017;8(16):26041-26056.
- Chien CS, Chen YH, Chen HL, et al. Cells responsible for liver mass regeneration in rats with 2-acetylaminofluorene/partial hepatectomy injury. *J Biomed Sci*. 2018;25(1):39.
- Bagnyukova TV, Tryndyak VP, Montgomery B, et al. Genetic and epigenetic changes in rat preneoplastic liver tissue induced by 2-acetylaminofluorene. *Carcinogenesis*. 2008;29(3):638-646.
- Ohlson LC, Koroxenidou L, Hällström IP. Inhibition of in vivo rat liver regeneration by 2-acetylaminofluorene affects the regulation of cell cycle-related proteins. *Hepatology*. 1998;27(3):691-696.
- Weber A, Boege Y, Reisinger F, Heikenwälder M. Chronic liver inflammation and hepatocellular carcinoma: persistence matters. *Swiss Med Wkly*. 2011;141:w13197.
- Schiffer E, Housset C, Cacheux W, et al. Gefitinib, an EGFR inhibitor, prevents hepatocellular carcinoma development in the rat liver with cirrhosis. *Hepatology*. 2005;41(2):307-314.
- Wu K, Ding J, Chen C, et al. Hepatic transforming growth factor beta gives rise to tumor-initiating cells and promotes liver cancer development. *Hepatology*. 2012;56(6):2255-2267.
- Sánchez-Rodríguez R, Torres-Mena JE, De-la-Luz-Cruz M, et al. Increased expression of prostaglandin reductase 1 in hepatocellular carcinomas from clinical cases and experimental tumors in rats. *Int J Biochem Cell Biol*. 2014;53:186-194.
- Jensen EC. Quantitative analysis of histological staining and fluorescence using ImageJ. *Anat Rec*. 2013;296(3):378-381.
- Livak KJ, Schmittgen TD. Analysis of relative gene expression data using real-time quantitative PCR and the 2(-delta delta C(T)) method. *Methods*. 2001;25(4):402-408.
- Mak KM, Mei R. Basement membrane type IV collagen and laminin: an overview of their biology and value as fibrosis biomarkers of liver disease. *Anat Rec*. 2017;300(8):1371-1390.
- Dewidar B, Meyer Do oley, Meindl-Beinker. TGF- β in hepatic stellate cell activation and liver fibrogenesis-updated 2019. *Cells*. 2019;8(11).
- Hendrich S, Pitot HC. Enzymes of glutathione metabolism as biochemical markers during hepatocarcinogenesis. *Cancer Metastasis Rev*. 1987;6(2):155-178.
- Sakai M, Muramatsu M. Regulation of glutathione transferase P: a tumor marker of hepatocarcinogenesis. *Biochem Biophys Res Commun*. 2007;357(3):575-578.
- Ye F, Jing YY, Guo SW, et al. Proliferative ductular reactions correlate with hepatic progenitor cell and predict recurrence in HCC patients after curative resection. *Cell Biosci*. 2014;4(1):50.
- Yovchev MI, Grozdanov PN, Joseph B, Gupta S, Dabeva MD. Novel hepatic progenitor cell surface markers in the adult rat liver. *Hepatology*. 2007;45(1):139-149.
- Williams GM, Iatropoulos MJ, Jeffrey AM. Thresholds for the effects of 2-acetylaminofluorene in rat liver. *Toxicol Pathol* (2004;32(Suppl 2):85-91.
- Gerlyng P, Grotmol T, Seglen PO. Effect of 4-acetylaminofluorene and other tumour promoters on hepatocellular growth and binucleation. *Carcinogenesis*. 1994;15(2):371-379.
- Malik S, Bhatnagar S, Chaudhary N, Katare DP, Jain SK. DEN+2-AAF-induced multistep hepatotumorigenesis in Wistar rats: supportive evidence and insights. *Protoplasma*. 2013;250(1):175-183.
- Chen J, Zhang X, Xu Y, et al. Hepatic progenitor cells contribute to the progression of 2-acetylaminofluorene/carbon tetrachloride-induced cirrhosis via the non-canonical Wnt pathway. *PLoS One*. 2015;10(6):e0130310.
- Trautwein C, Will M, Kubicka S, Rakemann T, Flemming P, Manns MP. 2-acetaminofluorene blocks cell cycle progression after hepatectomy by p21 induction and lack of cyclin E expression. *Oncogene*. 1999;18(47):6443-6453.
- Pogribny IP, Muskhelishvili L, Tryndyak VP, Beland FA. The role of epigenetic events in genotoxic hepatocarcinogenesis induced by 2-acetylaminofluorene. *Mutat Res*. 2011;722(2):106-113.
- Gordon GJ, Coleman WB, Grisham JW. Temporal analysis of hepatocyte differentiation by small hepatocyte-like progenitor cells during liver regeneration in retrorsine-exposed rats. *Am J Pathol*. 2000;157(3):771-786.
- Singal AG, El-Serag HB. Hepatocellular carcinoma from epidemiology to prevention: translating knowledge into practice. *Clin Gastroenterol Hepatol*. 2015;13(12):2140-2151.
- Caviglia JM, Schwabe RF. Mouse models of liver cancer. *Methods Mol Biol*. 2015;1267:165-183.
- Lorenzini S, Bird TG, Boulter L, et al. Characterisation of a stereotypical cellular and extracellular adult liver progenitor cell niche in rodents and diseased human liver. *Gut*. 2010;59(5):645-654.
- Ho DWY, Yang ZF, Yi K, et al. Gene expression profiling of liver cancer stem cells by RNA-sequencing. *PLOS One*. 2012;7(5):e37159.
- Andersen JB, Loi R, Perra A, et al. Progenitor-derived hepatocellular carcinoma model in the rat. *Hepatology*. 2010;51(4):1401-1409.
- Sánchez-Rodríguez R, Torres-Mena JE, Quintanar-Jurado V, et al. Ptgr1 expression is regulated by NRF2 in rat hepatocarcinogenesis and promotes cell proliferation and resistance to oxidative stress. *Free Radic Biol Med*. 2017;102:87-99.
- Lowes KN, Brennan BA, Yeoh GC, Olynyk JK. Oval cell numbers in human chronic liver diseases are directly related to disease severity. *Am J Pathol*. 1999;154(2):537-541.
- Torres-Mena JE, Salazar-Villegas KN, Sánchez-Rodríguez R, et al. Aldo-Keto reductases as early biomarkers of hepatocellular carcinoma: a comparison between animal models and human HCC. *Dig Dis Sci*. 2018;63(4):934-944.
- Tummala KS, Brandt M, Teijeiro A, et al. Hepatocellular carcinomas originate predominantly from hepatocytes and benign lesions from hepatic progenitor cells. *Cell Rep*. 2017;19(3):584-600.

40. Xu XD, Shao SX, Jiang HP, et al. Warburg effect or reverse Warburg effect? A review of cancer metabolism. *Oncol Res Treat.* 2015;38(3):117-122.
41. Wilde L, Roche M, Domingo-Vidal M, et al. Metabolic coupling and the reverse Warburg effect in cancer: implications for novel biomarker and anticancer agent development. *Semin Oncol.* 2017;44(3):198-203.
42. Sangineto M, Villani R, Cavallone F, Romano A, Loizzi D, Serviddio G. Lipid metabolism in development and progression of hepatocellular carcinoma. *Cancers.* 2020;12(6):1419.
43. Guimaraes JC, Zavolan M. Patterns of ribosomal protein expression specify normal and malignant human cells. *Genome Biol.* 2016;17(1):236.
44. Petkov PM, Zavadil J, Goetz D, et al. Gene expression pattern in hepatic stem/progenitor cells during rat fetal development using complementary DNA microarrays. *Hepatology.* 2004;39(3):617-627.

SUPPORTING INFORMATION

Additional Supporting Information may be found online in the supporting information tab for this article.

How to cite this article: Castro-Gil MP, Sánchez-Rodríguez R, Torres-Mena JE, et al. Enrichment of progenitor cells by 2-acetylaminofluorene accelerates liver carcinogenesis induced by diethylnitrosamine in vivo. *Molecular Carcinogenesis.* 2021;60:377-390.
<https://doi.org/10.1002/mc.23298>